3-D Mapping of Solids Flow Fields in Multiphase Reactors with RPT

Faïçal Larachi and Jamal Chaouki
Dept. of Chemical Engineering, École Polytechnique de Montréal, Montréal, Canada, H3C 3A7

Gregory Kennedy
Nuclear Engineering Inst., École Polytechnique de Montréal, Montréal, Canada H3C 3A7

Recent important progress in the field of multiphase flows is due to the implementation of noninvasive remote imaging and flow visualization techniques, which were developed in such fields as nuclear medicine, physics and fluid mechanics. Aided by spectacular improvements in computer performance, these techniques have contributed to the increased interest in the investigation of multiphase chemical reactor hydrodynamics. Their advantage over probe techniques, besides being noninvasive, is that they provide a full picture of the flow field for the phase studied rather than local information in the vicinity of the probe. The high degree of spatial and temporal resolution achievable more than justifies the additional complexity of the measurements.

Nuclear-based remote imaging techniques, such as X-ray and thermal neutron transmission tomography, have been used to obtain images of voidage fields in consolidated porous media (Jasti and Fogler, 1992), moving granular beds (Hosseini-Ashrafi and Tüzün, 1993) and gas-liquid pipe flows (Modi et al., 1992). Gas holdup field imaging in bubble columns using gamma-ray transmission tomography (CAT) is currently being used by the Duduković group (Yang et al., 1993). Tomographic techniques, however, usually provide information only on the flow morphology and not on the motion of the flowing phases, which explains why velocity field measurements have been unavailable. Hence, the last decade has seen an intensified effort to develop new nuclear-based techniques specifically suited to velocity field mapping in flowing systems. The dynamic NMR imaging technique has recently been used to map the velocity field of a laminar single fluid flow in different geometries (Xia et al., 1992; Chung et al., 1993). Positron emission particle tracking (PEPT), based on the detection of annihilation photons, has been applied to studies of powder velocity fields in rotary mixers and in gas-solid fluidized beds (Parker et al., 1993). Computer-automated radioactive particle tracking (CARPT), based on the detection of high energy gamma rays emitted by a radioisotope-labeled solid particle, enabled velocity field measurements for the solids in gas-solid fluidized beds (Lin et al., 1985; Moslemian et al., 1989; Devanathan and Moslemian, 1988) and for the liquid in bubble columns (Devanathan et al., 1990; Duduković et al., 1991; Yang et al., 1992a,b, 1993; Duduković and Devanathan, 1993).

This article describes a new radioactive particle tracking system (RPT) developed for mapping solids velocity fields in multiphase reactors by tracking a gamma-emitting particle that follows the solid phase. In principle, the method is similar to CARPT (Duduković et al., 1991), but it should yield improved spatial resolution because of the use of a model which accurately describes the interactions of the gamma rays with the reactor and the detectors and a least-squares 3-D (three-dimensional) inverse reconstruction algorithm. The new technique is currently being used to map the mean Eulerian solids velocity fields in three-phase fluidized beds (Larachi et al., 1993a) and in gas-solid spouted beds (Roy et al., 1994), and soon will be operational on circulating and turbulent gas-solid fluidized beds.

Detection System and Method of Calculation of Tracer Position

Figure 1 shows a typical arrangement of the detectors around the reactor where they are placed on two levels of four surrounding the column with 90° spacing. A flow follower of the same size and density as the solids in the reactor is tagged with the radioisotope ^{46}Sc. It emits gamma rays of energies 889 and 1,120 keV that are continuously monitored by an array of eight uncollimated 76 mm × 76 mm Tl activated sodium iodide scintillation detectors (energy resolution, 7.5%). A multiscaling system acquires data simultaneously for the eight detectors. Energy discrimination ensures that only signals corresponding to full gamma ray energy deposited in the detector are counted. The count rates recorded by the eight detectors are used to determine the tracer position.

Correspondence concerning this article should be addressed to J. Chaouki.

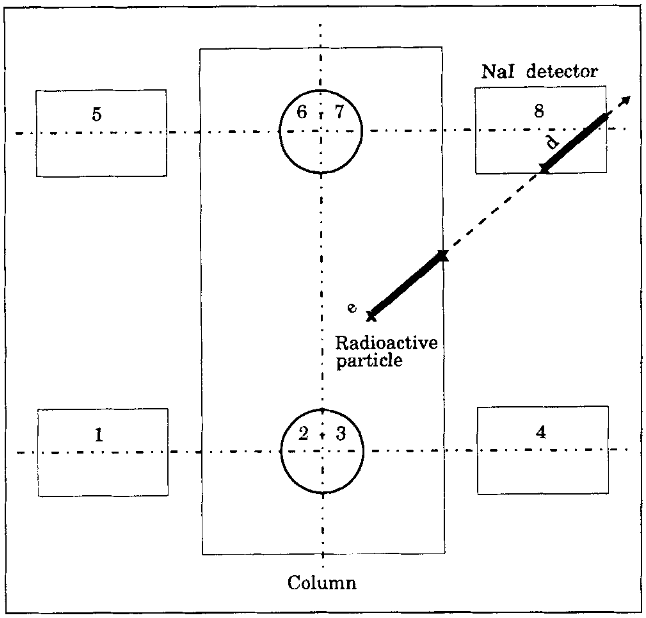

Figure 1. Arrangement of detectors around the reactor and geometrical construction determining path length *e* and distance *d* traveled by the photons in the reactor and detector.

The number of photopeak counts C recorded by the scaler during time T from a source of activity A placed in a dense medium at (x, y, z), a certain distance away from a detector, depends on: (1) the probability that a gamma ray emitted towards the detector will emerge from the reactor without being absorbed or scattered; (2) the absolute total full-energy peak efficiency of the detector, that is, the fraction of unscattered gamma rays emerging from the reactor which are recorded.

Quantitatively, this dependence can be expressed according to the following relationship (Tsoulfanidis, 1983):

$$C=\frac{T\nu A\phi \int\int_{\{\Omega\}} \frac{\vec{r}\cdot\vec{n}}{r^3} \exp(-\mu_R e)[1-\exp(-\mu_D d)]d\Sigma}{1+\tau\nu A\phi \int\int_{\{\Omega\}} \frac{\vec{r}\cdot\vec{n}}{r^3} \exp(-\mu_R e)[1-\exp(-\mu_D d)]d\Sigma} \quad (1)$$

where ν is the number of gamma rays emitted per disintegration ($\nu=2$ for ^{46}Sc), r is the distance between the source and a point on the outer surface of the crystal, e the path length traveled by the gamma ray in the reactor and d the thickness of the crystal in the direction given by vector $\vec{r}$ (Figure 1). ϕ is the peak-to-total ratio and τ the dead time per recorded pulse.

Gamma rays which Compton scatter in the reactor are rejected by the discriminators and do not contribute to the accepted (photopeak) counts. They do, however, contribute to the dead time, but their omission from the denominator of Eq. 1 is justified by the fact that the dead time correction is high only when the source is near the detector. This is where the unscattered gamma rays impinging on the detector far outnumber the scattered ones (Larachi et al., 1994).

Equation 1 cannot be solved analytically for a complicated geometry such as the one shown in Figure 1. It is evaluated numerically using a Monte Carlo calculation which models the emission, attenuation and detection of the gamma rays (Larachi et al., 1994). The Monte Carlo calculations are verified by comparing the calculated counts for the eight detectors with those measured by placing the radioactive particle at 150 locations under actual flow conditions via the calibration ports. Then, for each detector, a map is computer-generated using the Monte Carlo calculation for approximately 20,000 grid points throughout the reactor.

The inverse operation consists of locating the *a priori* unknown tracer position using the measured counts in each detector. A given number of counts in one detector implies that the particle is located on an isocount shell, which is a sphere distorted by the attenuation of the dense medium in the reactor and by the anisotropicity of the detector. The actual tracer position is at the intersection of the eight isocount shells corresponding to the eight detectors. These shells are imprecise and a strategy must be adopted to calculate the optimal intersection point, because of the statistical fluctuations inherent in the measured counts. The least-squares approach which was adopted searches among the 20,000 grid points to find the one which minimizes the weighted sum over the eight detectors of the squares of the differences between the measured counts and the Monte Carlo calculations. Since the coordinates of the best grid point thus determined are not of sufficient accuracy, the search is continued in the neighborhood of this point. It is not necessary to perform new Monte Carlo calculations for each new point tested because, for small variations in position, no accuracy is lost if it is assumed that the detector efficiency varies as the inverse square of the distance between the source and the center of the detector. In this case Eq. 1 can be replaced by:

$$C^*=\frac{TC\left(\frac{r}{r^*}\right)^2 \exp[\mu_R(e-e^*)]}{T-\tau C+\tau C\left(\frac{r}{r^*}\right)^2 \exp[\mu_R(e-e^*)]} \quad (2)$$

Here the symbols with asterisks refer to the new location and the others to the nearby grid point, r is the distance between the source and the geometric center of the detector and e is the path length traversed by the gamma ray through the dense medium along r.

Performance of the System

In order to measure the accuracy and precision of the system for determining the tracer location, tests were performed under actual flow conditions in both the spouted bed and the fluidized bed with a static tracer positioned at known locations and a moving tracer constrained to a concentric circular trajectory. The resolution of the system can be quantified in terms of spatial standard deviations which should be as small as possible. One expects the following relationship between the 3-D standard deviation and the system characteristics (Bevington, 1969):

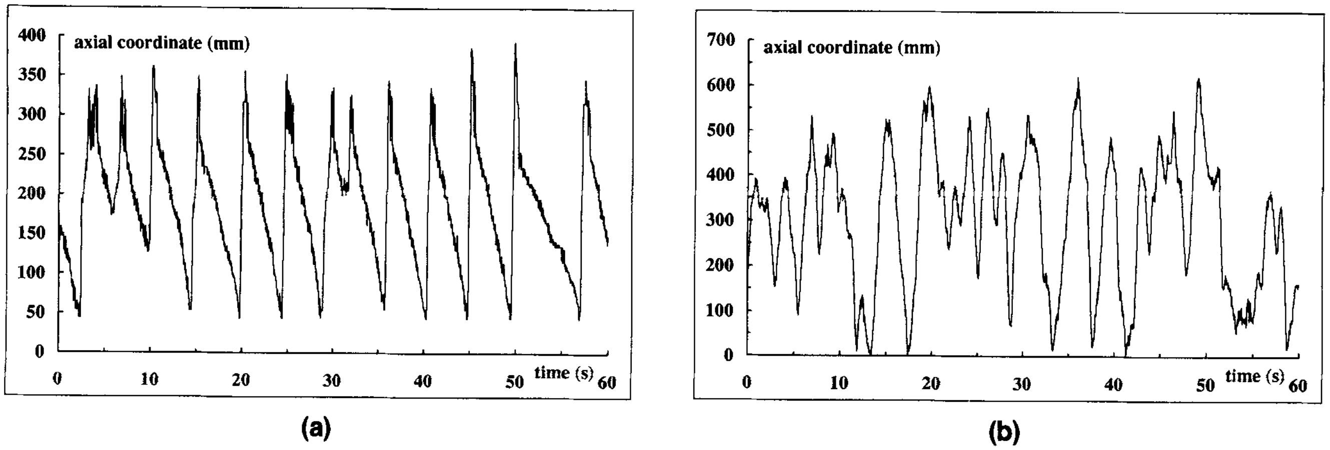

Figure 2. Tracking of labeled tracer particle (a) in a gas-solid spouted bed and (b) in a three-phase fluidized-bed variation with time of axial component.

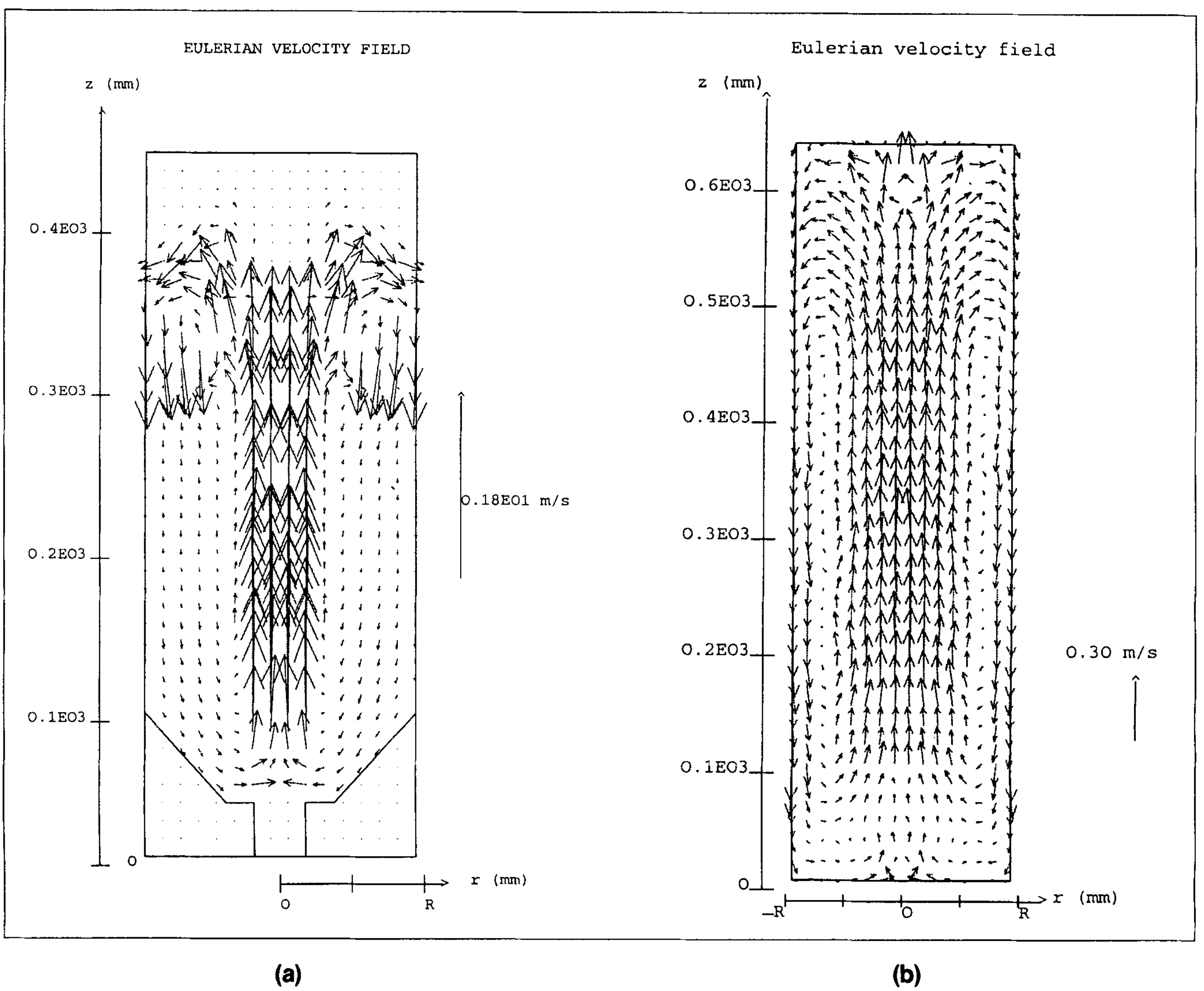

Figure 3. Mean Eulerian velocity field of the axisymmetrical solids flow (a) in a gas-solid spouted bed and *(b) in a* three-phase fluidized bed.

$$\sigma_{3\text{-}D}^2=\sigma_x^2+\sigma_y^2+\sigma_z^2=\frac{1}{\Sigma_1^8 C_i\left(\frac{\partial \ln C_i}{\partial x}\right)^2}+\frac{1}{\Sigma_1^8 C_i\left(\frac{\partial \ln C_i}{\partial y}\right)^2}+\frac{1}{\Sigma_1^8 C_i\left(\frac{\partial \ln C_i}{\partial z}\right)^2} \quad (3)$$

It has been demonstrated previously (Larachi et al. 1993b, 1994) that the spatial resolution is improved by: (1) increasing the number of detectors; (2) reducing the distance between the column walls and the detectors; and (3) increasing the sampling time. The resolution was, however, independent of the density of the reactor fluid mixtures. For the 0.03-s sampling period, the average 3-D standard deviation varied from 3 to 8 mm (average 6 mm) for both the fluidized and the spouted beds with a 1.85-MBq radioactive source and 8 detectors surrounding 500–800-mm-high emulsions. With the same sampling period and 16 detectors, Devanathan (1991) reported resolutions of up to 26 mm for empty columns and even greater for fluid-filled columns.

Application to Solids Velocity Field in Three-Phase Fluidized and Gas-Solid Spouted Beds

As an illustration of the performance of the system in a real situation, Figure 2 shows the movement in the axial direction (vertical) of a tagged particle, activity 1.85 MBq, in a gas-solid spouted bed with conical base and a three-phase fluidized bed both containing 3-mm glass beads. The sharp peaks in Figure 2a indicate very fast movement in the spout region where velocities as high as 2 m/s are measured. The movement is very regular and a mean circulation time of the solid particles can easily be determined. It may also be seen that the particles descend with an annular downward flow, and most of the time they reach the bottom of the reactor where they are pushed up by the gas in the upward spout flow (Roy et al., 1994). In the three-phase fluidized bed, the solid flow (Figure 2b) is less regular than in the spouted bed. However, several long and slightly irregular trajectories can be observed. Large ascending bubbles may drift and their wakes may convectively entrain solid particles from the distributor to the bed inversion zone, because of the prevailing heterogeneous flow in the bed. Velocity fields can be plotted in a 2-D r-z frame as shown in Figures 3a and 3b for the spouted bed and the fluidized bed, because of the axial symmetry of the flows. Each velocity vector shown is the average of all velocities determined at a given location, and details on velocity calculations may be found in Duduković et al. (1991).

The improved analysis and flow diagnosis of the multiphase hydrodynamics made possible by the present technique will lead to a more profound understanding of the phenomena involved in the motion of discrete particles in multiphase reactors. The technique will soon be implemented on circulating and turbulent gas-solid fluidized beds.

Acknowledgments

The authors gratefully acknowledge financial support from the Natural Sciences and Engineering Research Council of Canada. Thanks are also addressed to Dr. M. Cassanello and D. Roy for their contribution to this work.

Notation

A = source activity, MBq
C = gamma ray count
d = distance traversed in the crystal by an undisturbed gamma ray, mm
e = path length traveled in the reactor by an undisturbed gamma ray, mm
r = distance between source and a point on the outer surface of the crystal, mm
T = sampling time, s
x = horizontal coordinate, mm
y = horizontal coordinate, mm
z = vertical coordinate, mm

Greek letters

σ = standard deviation, mm
τ = detector dead time, s
μ = total linear attenuation coefficient, mm^{-1}
Ω = solid angle, strd

Subscripts

D = detector
R = reactor

Literature Cited

Bevington, P. R., *Data Reduction and Error Analysis for the Physical Sciences*, McGraw-Hill, New York (1969).

Chung, K. Y., G. Belfort, W. A. Edelstein, and X. Li, "Dean Vortices in Curved Tube Flow: 5. 3-D MRI and Numerical Analysis of the Velocity Field," *AIChE J.*, **39**, 1592 (1993).

Devanathan, N., and D. Moslemian, "A PC Based Data Acquisition System for Investigation of Phase Recirculation in Multiphase Systems," *Symp. Small Comp. Fluid Mech.*, ASME Meeting, Chicago, p. 53 (1988).

Devanathan, N., D. Moslemian, and M. P. Duduković, "Flow Mapping in Bubble Columns using CARPT," *Chem. Eng. Sci.*, **45**, 2285 (1990).

Devanathan, N., "Investigation of Liquid Hydrodynamics in Bubble Columns via Computer-Automated Radioactive Particle Tracking (CARPT)," DSc, St. Louis, MO (1991).

Duduković, M. P., N. Devanathan, and R. Holub, "Multiphase Reactors: Models and Experimental Verification," *Rev. Inst. Franç. Pétr.*, **46**, 439 (1991).

Duduković, M. P., and N. Devanathan, "Bubble Column Reactors: Some Recent Developments," *Chemical Reactor Technology for Environmentally Safe Reactors and Products*, H. I. de Lasa, G. Doğu, and A. Ravella, eds., NATO ASI Ser. E: Appl. Sci., **225**, p. 353 (1993).

Hosseini-Ashrafi, M. E., and U. Tüzün, "A Tomographic Study of Voidage Profiles in Axially Symmetric Granular Flows," *Chem. Eng. Sci.*, **48**, 53 (1993).

Jasti, J. K., and H. S. Fogler, "Applications of Neutron Radiography to Image Flow Phenomena in Porous Media," *AIChE J.*, **38**, 481 (1992).

Larachi, F., J. Chaouki, C. Guy, and G. Kennedy, "Solids Mixing Investigation in a Three-Phase Fluidized Bed," CHISA, Session I1, paper 560, Prague, Czech Republic (Aug. 29–Sept. 3, 1993a).

Larachi, F., J. Chaouki, and G. Kennedy, "Poursuite Assistée par Ordinateur de Traceurs Radioactifs dans les Réacteurs Polyphasiques," *Récents Progrès en Génie des Procédés*, C. Jallut, ed., Techniques et Documentation, Lavoisier, Paris, France, **27**, p. 397 (1993b).

Larachi, F., G. Kennedy, and J. Chaouki, "A γ-Ray Detection System for 3-D Particle Tracking in Multiphase Reactors," *Nucl. Instr. and Meth.*, **A**, **338**, 568 (1994).

Lin, J. S., M. M. Chen, and B. T. Chao, "A Novel Radioactive Particle Tracking Facility for Measurement of Solids Motion in Gas Fluidized Beds," *AIChE J.*, **31**, 465 (1985).

Modi, V., C. Gnafakis, and C. C. Gryte, "Experiments with Computed X-Ray Tomography to Observe Horizontal Two-Phase Pipe Flow," *Chem. Eng. Comm.*, **116**, 117 (1992).

Moslemian, D., M. M. Chen, and B. T. Chao, "Experimental and Numerical Investigations of Solids Mixing in a Gas-Solid Fluidized Bed," *Part. Sci. Technol.*, 7, 335 (1989).

Parker, D. J., C. J. Broadbent, P. Fowles, M. R. Hawkesworth, and P. McNeil, "Positron Emission Particle Tracking—A Technique for Studying Flow within Engineering Equipment," *Nucl. Instr. and Meth.*, **A326**, 592 (1993).

Roy, D., F. Larachi, R. Legros, and J. Chaouki, "A Study of Solid Behavior in Spouted Beds Using 3-D Particle Tracking," *Can. J. Chem. Eng.*, **72**, 945 (1994).

Tsoulfanidis, N., *Measurement and Detection of Radiation*, Series in Nuclear Engineering, McGraw-Hill, New York (1983).

Xia, Y., P. T. Callaghan, and K. R. Jeffrey, "Imaging Velocity Profiles: Flow through an Abrupt Contraction and Expansion," *AIChE J.*, **38**, 1403 (1992).

Yang, Y. B., N. Devanathan, and M. P. Duduković, "Liquid Backmixing in Bubble Columns via Computer Automated Particle Tracking (CARPT)," AIChE Meeting, Miami Beach, FL (Nov. 1-6, 1992a).

Yang, Y. B., N. Devanathan, and M. P. Duduković, "Liquid Backmixing in Bubble Columns via Computer Automated Particle Tracking (CARPT)," *Chem. Eng. Sci.*, **47**, 2859 (1992b).

Yang, Y. M. P., B. S. Zou, and M. P. Duduković, "Liquid Backmixing in Bubble Columns using Computer Automated Particle Tracking (CARPT)," AIChE Meeting, St. Louis, MO (Nov. 6-12, 1993).

Manuscript received Dec. 3, 1993, and revision received Feb. 23, 1994.